Investigation of Diagnostic Techniques for Metal Oxide Surge Arresters

K. P. Mardira, T. K. Saha
School of Information Technology & Electrical Engineering
University of Queensland, Brisbane, Qld 4072, Australia

and R. A. Sutton
Division of Materials, School of Engineering
University of Queensland, Brisbane, Qld 4072, Australia

ABSTRACT

Gapless metal oxide surge arresters (MOSA) have been available in the market for many years since they were first introduced in the 1970's. The aim of this study is to investigate some reliable diagnostic techniques to assess the condition of a metal oxide surge arrester when subjected to severe lightning strikes in the field. A number of non-destructive and destructive diagnostic techniques for Metal Oxide Surge Arrester (MOSA) are discussed in this paper. The non-destructive techniques include the standard 1 mA reference voltage, lightning impulse discharge residual voltage and a number of modern diagnostics based on polarization methods: Return voltage and polarization/depolarization current measurements. In order to observe, analyze and correctly explain the degradation phenomena, a number of destructive techniques based on microstructure observation are also conducted. The techniques include optical microscopy, scanning electron microscopy, X-Ray diffraction and energy dispersive spectrometry. The single and multi-pulse currents of 8/20 μs wave shape were used to artificially degrade the MOSA. The before and after diagnostic results of the non-destructive and destructive techniques are presented and interpreted to understand the aging mechanism in MOSA. The importance of modern non-destructive electrical diagnostics based on polarization methods is validated by test results and is highlighted in detail in this paper. Finally the correlation of the results of different diagnostic techniques with each other and with the results of standard techniques is discussed.

Index Terms — **Metal oxide surge arrester, aging by lightning impulse currents, degradation mechanism, polarization/depolarization current, return voltage, optical microscopy, scanning electron microscopy, X-Ray diffraction, energy dispersive spectrometry.**

1 INTRODUCTION

THE gapless metal oxide surge arresters (MOSA) have been available in the market for many years since they were first introduced in the 1970's. Its primary function is to protect the equipment in the system against various electrical overstresses. The protection level of MOSA was rapidly developed to meet the withstand requirements such as high-energy absorption capability, current withstand level and voltage stress. However, these fast developments are not accompanied by the development of better techniques to assess the condition of MOSA after being subjected to heavy stress from ac and lightning impulse currents. It is known that current-voltage characteristics of metal oxide varistors become degraded due to the continuous application of ac or due to transients with currents larger than the varistors ratings. It is believed that degradation mainly affects the pre-breakdown region of the I-V curve and results in increased leakage currents [1]. To test for any such degradation manufacturers normally apply single pulse 8/20 μs lightning transients at the rated current of the device. However, it is now known that most lightning ground flashes consist of multiple return strokes. A typical flash consists of four pulses within 1 s with time intervals of about 40 ms between pulses [1]. Darveniza et al. [2] investigated the effects of multiple pulse lightning

Manuscript received on 2 September 2003, in final form 6 May 2004.

currents on metal oxide surge arresters and showed that the damage caused is not normally evident with standard lightning current tests. Many existing standards (Australian Standard, IEC, ANSI, etc) [3–5] in general only provide the criteria for pass/fail condition of MOSA by using before and after diagnostic results from the lightning current impulse applications without knowing their degree of degradation.

Many investigations of field aged cables and transformers have reported meaningful interpretations of the condition of the insulation by using new diagnostic techniques. Return voltage measurement and polarization/depolarization current measurement have been increasingly used. Since a MOSA is an insulator at normal conditions (below its rated voltage), the effect of polarization and depolarization of its dipole within the insulation can be monitored by any of these polarization based diagnostics. Monitoring the condition of a MOSA can be better understood by observing and analyzing the degradation phenomena in micrometer or sub-micrometer scale. Destructive diagnostic techniques based on microstructure observation, such as optical microscopy, scanning electron microscopy, X-Ray diffraction, and energy dispersive spectrometry are powerful techniques to observe and characterize solid objects on a small scale.

A number of distribution class MOSA was first artificially degraded by single and multi-pulse lightning impulse currents of 8/20 μs wave shape with higher magnitude than the ratings of the arrester. In this paper, a number of non-destructive and destructive diagnostic techniques are discussed and their relevant test procedures including specimen preparation for damage assessment are presented. The findings from these systematic experiments with the purpose to assess the condition of the arresters after such severe degradations are described in this paper. The results from the non-destructive and destructive techniques are compared and discussed in detail. Finally, this paper presents the interpretation of different diagnostic results and their correlation to a number of existing diagnostic methods to better explain the degradation mechanism of a metal oxide surge arrester.

2 THEORY

2.1 NON-DESTRUCTIVE TECHNIQUES

2.1.1 1 MA REFERENCE VOLTAGE MEASUREMENT

The level of degradation can be determined by measuring the complete I-V characteristics or at least one I–V check point conveniently near the nominal voltage of the varistor. In this investigation the latter technique is used to study the effect of application of current pulses on a MOSA. The ac reference voltage is measured, which is the voltage required to pass the 1 mA leakage current through the arrester. This reference current value refers to the peak of the resistive current component (the higher peak of the two polarities if the current is not symmetrical). This measurement is performed at an ambient temperature of 25 ± 10°C [3].

Diagnostic tests for an arrester which are performed before the application of a lightning impulse current are known as "before diagnostics". The repeated diagnostic or the so called "after diagnostic" is performed following the degradation process by the application of a number of lightning impulse currents and is used for comparison with the "before diagnostic" result. Australian Standard AS 1307.2 recommends that the change of ac reference voltage should not be more than $\pm 5\%$ for a good MOSA [3]. This simply describes a good/pass condition of an arrester.

2.1.2 DISCHARGE RESIDUAL VOLTAGE MEASUREMENT

The second method to assess the pass/fail condition is to measure the discharge residual voltage at nominal rated discharge current. This measurement is performed to obtain the maximum residual voltage for a given design for all specified currents and wave shapes. In AS.1307.2, a 8/20 μs current impulse is used with limits on the adjustment of equipment such that the measured values are from 7 to 9 μs for the virtual front time and from 18 to 22 μs for the time to half value on the tail [6]. However, the time to half is not critical and may have any tolerance during a residual type test [3].

Three current impulses are applied to each arrester sample with peak current values of approximately 0.8, 1.0 and 1.2 times the nominal rated discharge current of the arrester. A sufficient time interval between the discharges is maintained to permit the sample to return to approximately ambient temperature. The criteria specified by AS. 1307.2 for assessing the condition of an arrester include no physical damage to arrester to be seen and the change not greater than $\pm$ 5 % of residual voltage between the before and after diagnostic tests.

2.1.3 POLARIZATION/DEPOLARIZATION CURRENT MEASUREMENT

This method is to quantify the dielectric response of the insulating materials by allowing observation of the polarization development in time when a step voltage is applied. When a step voltage of magnitude U_0 is applied to an initially uncharged dielectric, the polarization current flowing through it is given by (1). The process is summarized in Figure 1.

$$i_p(t) = C_0 U_0 \left[\frac{\sigma}{\epsilon_0} + f(t) \right] \quad (1)$$

Where σ is the dc conductivity, ϵ_0 is the permittivity of vacuum, $f(t)$ is the response function and C_0 is the geo-

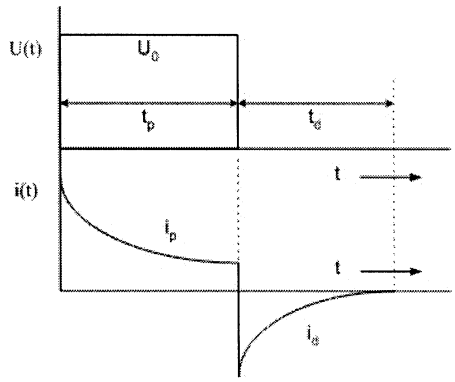

Figure 1. Waveform of polarization and depolarization currents.

metric capacitance (measured capacitance divided by relative permittivity) of the dielectric material. Once the step voltage is replaced by a short circuit, a depolarization current is built up. The depolarization current is expressed as:

$$i_d(t) = -C_0U_0\left[f(t) - f(t+t_p)\right] \tag{2}$$

It has been shown [7] that, for an oil/cellulose insulation system of a transformer the 'dielectric response function' can be expressed in parametric form as:

$$f(t) = \frac{A}{\left(\frac{t}{t_0}\right)^n + \left(\frac{t}{t_0}\right)^m} \tag{3}$$

with A, $t_0 > 0$, $m > n > 0$ and $m > 1$.

However, we found that the response function $f(t)$ for the MOSA can be expressed in a general expression following the universal relaxation law, which is also found in many other experimental observations [8].

$$f(t) = mt^{-n} \tag{4}$$

In order to estimate the dielectric response function $f(t)$ from a depolarization current measurement it is assumed that the dielectric response function is a continuously decreasing function in time, then if the polarization period is sufficiently long, so that $f(t + t_p) \cong 0$, the dielectric response function $f(t)$ is proportional to the depolarization current. Thus from (2), the dielectric response function $f(t)$ can be approximated as

$$f(t) \approx \frac{-i_d(t)}{C_0U_0} \tag{5}$$

From the measurements of polarization and depolarization currents, it is possible to estimate the dc conductivity σ of the test object. If the test object is charged for a sufficiently long time so that $f(t + t_p) \cong 0$, (1) and (2) can be combined to express the dc conductivity of the dielectric as

$$\sigma \approx \frac{\epsilon_0}{C_0U_0}\left(i_p(t) - i_d(t)\right) \tag{6}$$

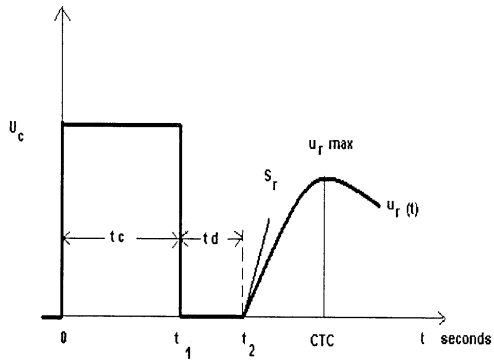

Figure 2. The Return Voltage phenomena.

2.1.4 RETURN VOLTAGE MEASUREMENT

Return voltage (RV) measurement is now increasingly used in the diagnosis of insulating materials for cables and transformers. Since a metal oxide surge arrester is an insulator at normal conditions (below its rated voltage), the effect of return voltage can also be monitored for a MOSA. The return voltage is based on the polarization and subsequent depolarization of dipoles within the insulating material as well as on the charging and discharging of grain boundaries and space charge effect [9, 10].

The return voltage measurement comprises three steps. Figure 2 shows the typical steps of return voltage.

1. Charge the test object for a pre-selected time (t_c) with a DC voltage (U_c), which is much lower than the rated voltage.

2. Discharge the test object for a short period of time (normally half of the charging time, $t_d = {}^1\!/_2\ t_c$).

3. Measure the open circuit voltage built up across the object (U_r). This is the return voltage.

There are three important parameters obtained from RV measurements that may characterize the condition of insulation [11–14]. They are maximum return voltage (U_{rmax}), time to reach maximum return voltage (central time constant (CTC)) and the initial slope (slope of return voltage curve for the first few seconds S_r).

The polarization processes which were not totally relaxed during the grounding period will relax and give rise to a return voltage across the electrodes of the insulation. The return voltage U_r can be expressed with the following equations.

$$i_r(t) = \sigma U_r(t) + \epsilon_0\epsilon_r\frac{dU_r(t)}{dt} + \epsilon_0\frac{d}{dt}\int_{t_2}^{t}(t-\tau)U_r(\tau)d\tau \tag{7}$$

for $t_2 < t < \infty$ and $U_r(t = t_2) = 0$

With the current $i_r(t)$ being zero during the voltage measurement (open circuit), (7) can be re-written as

$$\sigma U_r(t) + \epsilon_0\epsilon_r\frac{dU_r(t)}{dt} + \epsilon_0\frac{d}{dt}\int_{t2}^{t}f(t-\tau)U_r(\tau)d\tau = 0 \tag{8}$$

2.2 DESTRUCTIVE TECHNIQUES [13, 14]

2.2.1 OPTICAL MICROSCOPY

This is a standard technique in observing the microstructure of solid materials. The materials were sectioned perpendicularly using a low speed diamond saw and subsequently mounted for grinding and polishing. The specimens were then ground on silicon carbide paper. It was necessary to polish, as a large amount of pullout occurred during sectioning and grinding.

After experimenting with various polishing techniques, it was found that the best results could be obtained by first using a stone Petridisc. This appears to minimise the amount of pullout while still removing sufficient quantities of material. The specimens were then polished using a Texmet wheel and diamond paste, finishing with 1 μm diamond paste. It was found that use of 0.25 μm alumina, while reducing the size of the final scratches, resulted in contamination of the surface. The specimens were then examined in the unetched state and then lightly etched using 10 (M) of NaOH. This etchant preferentially attacks the ZnO. The specimens were then examined under optical microscope.

2.2.2 SCANNING ELECTRON MICROSCOPY

The scanning electron microscopy (SEM) is a powerful technique, which permits the observation and characterization of heterogeneous organic and inorganic materials and surfaces on micrometer or sub-micrometer scale. The area to be examined is irradiated with a finely focused beam impinging on the specimen's surface. The signals picked up on the probe include secondary electrons, backscattered electrons, Auger electrons, characteristic x-rays and photons of various energies. They relate to specific emission volumes within the sample and can be used to examine many characteristics of the sample (composition, surface topography and crystallography) [15, 16].

In the SEM, the signals of greatest interest are the secondary and backscattered electrons, since these vary according to differences in surface topography as the electron beams sweep across the specimens. The secondary electron emission is confined to a volume near the beam's impact area, permitting images to be obtained at relatively high resolution. This allows for the examination and analysis of solid specimens in the order of 2 to 5nm (20 − 50 Å), which cannot be obtained on an optical microscope.

2.2.3 X-RAY DIFFRACTION

X-ray diffraction (XRD) is commonly used to investigate the structure of matter at the molecular level. The most common application is to identify unknown substances. The reference XRD patterns are recorded from a range of specimens and these are compared with the pattern from the unidentified substance pattern. The substance is identified if its pattern coincides with that of the reference pattern. The XRD analysis of the specimens is performed by scattering in which the X-rays were scattered by Cu atoms without any changes in wavelength [17]. The specimens are analyzed over a diffraction angular range of 5 to 90° at a scan rate of 1.5 minutes/degree with steps of 4°. Quantitative analysis of diffraction data is obtained using integrated peak areas.

2.2.4 ENERGY DISPERSIVE SPECTROMETRY

Energy dispersive spectrometry (EDS) is an attractive tool for qualitative x-ray microanalysis. The fact that the total spectrum of interest, from 0.1 keV to beam energy (e.g. 20 keV) can be acquired in a short time (10−100 s) allows for a rapid qualitative composition evaluation of the specimens. At a high level energy beam (10 − 20 keV) the EDS detector has higher efficiency (95%) thus the relative peak heights observed for the families of X-ray lines are close to the values expected for the signal as it is emitted from the specimens. This qualitative intensity can be compared to the pre-selected and known elements to obtain the intensity ratio. This ratio is then used to identify the composition of the specimens [15, 16].

3 EXPERIMENTAL SET UP

Distribution class metal oxide surge arresters of 10 kA ratings used for this study were commercial devices produced by one particular manufacturer. There were two different types of arresters- (i) Double block type: D1, D2, D3, D4 and (ii) Single block type: S1, S2, S3 and S4. Double block arresters were made of two block varistors and had a rated voltage of 12.5 kV. Single block arresters consisted of only one block and had a rated voltage of 6.3 kV. They were new arresters and had identical characteristics in terms of reference voltage, residual voltage, return voltage and polarization/depolarization currents. The experimental procedure is summarized as follows.

3.1 BEFORE DIAGNOSTICS

1. Reference voltages at 1 mA resistive ac current were measured for all test samples [2].

2. Residual voltages were measured at rated current (10 kA) of 8/20 μs wave shape. Figure 3 presents the residual test set up.

3. Return Voltage Measurement (RVM) was performed with the circuit diagram shown in Figure 4. During the charging process switch 1 is closed and switches 2 and 3 are in the open position. The dc voltage source is connected to the test object. During the time $t = t_p$ the charging current $i_p(t)$ as in equation (1) flows through the circuit. During the grounding (discharging) process switch 1 is open; switch 2 is closed while switch 3 remains open. The voltage source is now isolated from the test material. For the duration of the discharging time $t = t_d$ the test object is short circuited and grounded. The depolarization

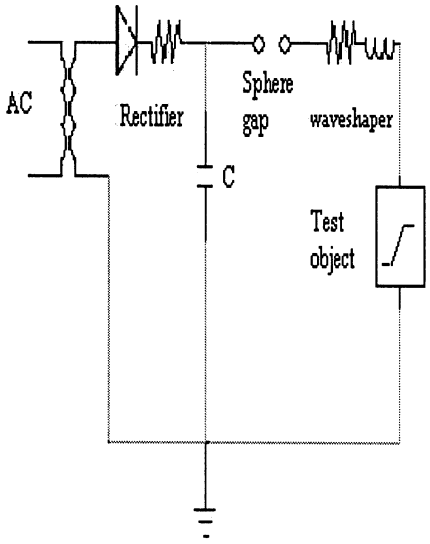

Figure 3. Residual Voltage Test Set Up.

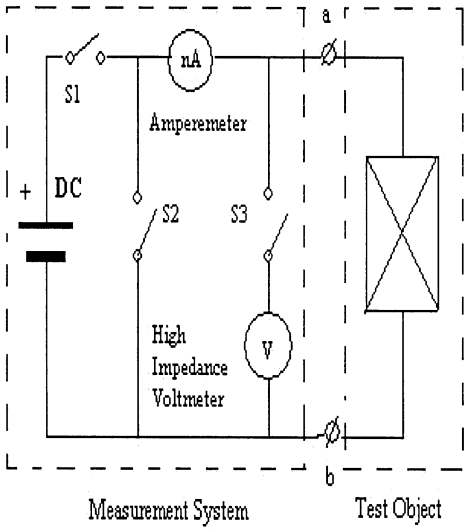

Figure 4. RVM Circuit Diagram.

current $i_{depol}(t)$ as in (2) will flow. The ratio between t_p/t_d is normally 2. The short circuit is then removed and the voltmeter measures the remaining voltage in the insulation. This is the so called "return voltage". This is done by keeping switches 1 and 2 open and closing switch 3. Return voltage measurement (RVM) was performed on all MOSAs with 1000 V_{dc}, 200 s charging time and 100 s discharging time. Automated computer controlled equipment developed at the University of Queensland was used for this measurement.

4. Polarization and depolarization currents measurement circuit diagram is shown in Figure 5. The basic circuit arrangement for the measurement of PDC of insulation consists of a high voltage source for charging the insulation and a sensitive current measuring device (Electrometer). It is recommended to use the 'two active electrodes' technique for the measurement. According to this technique, the insulation to be analyzed is connected between two electrodes. One of the electrodes is marked as the 'excitation electrode' and the test voltage is applied to it referenced to ground while the current is measured along a line connected between the second 'sensing electrode' and ground. With such a 'two active electrode' arrangement, effects of stray capacitances of the insulation to ground and also of cable capacitances can be reduced to a minimum. Polarization and depolarization currents were measured with 1000 V_{dc} and time for both sequences was 10^4 s.

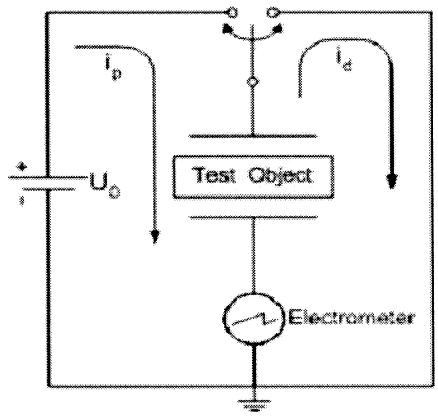

Figure 5. PDC Measurement.

5. Two terminals of the arresters were short circuited to ground for at least 24 h before the measurement of steps 3 and 4 were performed. This was done to eliminate the previous polarization effects (commonly known as memory effect), which normally affect the accuracy and reproducibility of the measurement.

6. Initial destructive diagnostics (steps are discussed in later part).

3.2 ARTIFICIAL DEGRADATION PROCESSES

MOSAs were systematically degraded as follows:

(a) Arresters D1, D2, S1 and S2 were subjected to 15 single pulse 8/20 μs lightning impulse current waveshapes at 2 p.u, 4 p.u., 2 p.u. and 4 p.u. with intervals of 1 minute plus time to charge the system respectively.

(b) Arresters D3 and S3 were subjected to 5 groups of multi-pulse currents at 1 p.u. while D4 and S4 were subjected to multi-pulse currents at 1.5 p.u. with small time intervals required to charge the system. The multi-pulse current test consisted of quintuple (5) 8/20 μs lightning current impulses with a time difference of 20-40 ms between each pulse [2, 18].

3.3 AFTER DIAGNOSTICS

Steps 1, 2, 3 and 4 were repeated for after diagnostic measurements.

3.4 DESTRUCTIVE DIAGNOSTICS

1. A section of each sample (varistors) was prepared for the micro-level observation:

a. MO varistors were first sectioned perpendicular to the contacts using a diamond saw, and subsequently mounted for grinding and polishing.

b. MO varistors were polished with 1 μm diamond paste.

c. MO varistors were then preferentially etched using 10M NaOH solution.

2. The Optical Microscopy of prepared MO varistors was performed.

3. Prepared MO varistors were analyzed using XRD.

4. The samples were then prepared for the SEM and EDS as follows:

a. Repeat step 1b and 1c,

b. Coat the specimen with carbon. This is to produce thin conductive films for electron microscopy. In this process, an energetic carbon ion is ejected under influence of applied voltage to the surface of a target from all angles.

c. Mount the carbon coated specimens to special stubs for SEM and EDS observations.

5. Carbon coated samples were then analyzed under the scanning electron probe and energy dispersive detector.

4 TEST RESULTS

The results from 1 mA reference voltage and discharge residual voltage measurements on the MOSA are presented in Tables 1 and 2, respectively. The changes in 1 mA reference voltage and residual voltage were within the allowable $\pm 5\%$ except for arrester D3. Arrester D3 had its residual voltage reduced by 5.6% and its 1mA reference voltage increased by more than 6 % of its original value. The results indicate that arrester D3 failed the standard test according to A.S.1307.2, while the other arresters passed.

Table 11. 1 mA reference voltage.

MOSA	1 mA ac reference voltage Before +ve and −ve	After +ve and −ve	Changes (%)
D1	13.1 and 13.3	13.4 and 13.7	2.3 and 3.1
D2	13.1 and 13.2	13.2 and 13.5	0.8 and 2.3
D3	13.1 and 13.2	13.8 and 14.1	5.3 and 6.8
D4	13.3 and 13.5	13.6 & 13.9	2.3 and 3.0
S1	6.7 and 6.9	7.0 and 7.1	4.3 and 2.9
S2	6.6 and 6.6	6.5 and 6.8	−1.5 and 3.0
S3	6.7 and 6.8	6.8 and 6.9	1.5 and 1.5
S4	6.8 and 6.9	7.0 and 7.1	3.0 and 2.9

Table 2. Residual voltage.

MOSA	Residual Voltage (kV) Before	After	Changes (%)
D1	34.7	33.0	−4.9
D2	34.6	33.0	−4.6
D3	35.6	33.6	−5.6
D4	35.4	34.3	−3.1
S1	18.1	17.8	−1.7
S2	18.1	17.7	−2.2
S3	18.0	17.8	−1.1
S4	18.1	17.8	−1.7

Table 3. Return voltage results.

(a) Return Voltage maximum value results.

MOSA	Return Voltage (V) Before	After	Changes (%)
D1	28.8	16.2	−43.8
D2	28.8	20.3	−29.5
D3	30.5	11.8	−61.3
D4	30.3	23.1	−23.8
S1	28.7	26.0	−9.4
S2	27.9	25.3	−9.3
S3	29.5	25.1	−14.9
S4	27.9	27.1	−2.9

(B) Central time constant results.

MOSA	Central time constant (s) Before	After	Changes (%)
D1	136.2	84.1	−38.9
D2	123.7	118.2	−4.4
D3	179.7	48.9	−72.8
D4	179.7	123.9	−31.1
S1	152.9	95.2	−37.7
S2	196.4	105.4	−46.3
S3	158.3	106.4	−32.8
S4	144.7	118.4	−18.2

Table 4. Polarization / depolarization results.

MOSA	dc Conductivity (σ) ($\times 10^{-12}$) S/m Before	After	Changes (%)
D1	1.70	1.94	14.1
D2	1.71	1.98	15.8
D3	1.74	2.48	42.5
D4	1.99	1.96	−1.5
S1	3.24	3.45	6.5
S2	3.51	3.82	8.8
S3	3.41	3.46	1.7
S4	3.37	3.46	2.7

Tables 3 and 4 present the results of the return voltage and polarization/depolarization current measurements, respectively. The average values of maximum return voltage and central-time constants are calculated for all similar arresters before degradation and are used as reference for comparison.

Table 3 (a and b) shows clearly that both the return voltage and the central-time constant for all arresters decreased after various current impulses. Arrester D3 showed the most significant change. It had its return voltage reduced to 39% of its original value and reached the peak voltage faster than its initial central-time constant. Arrester D1 showed the second largest reduction in its return voltage and central-time constant.

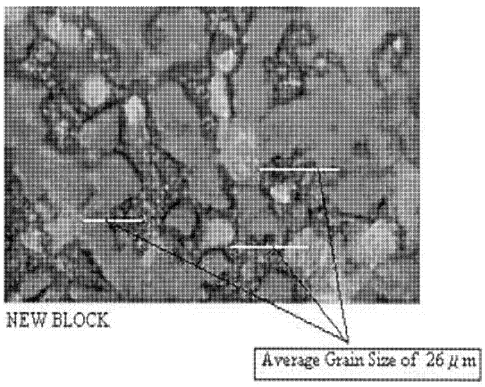

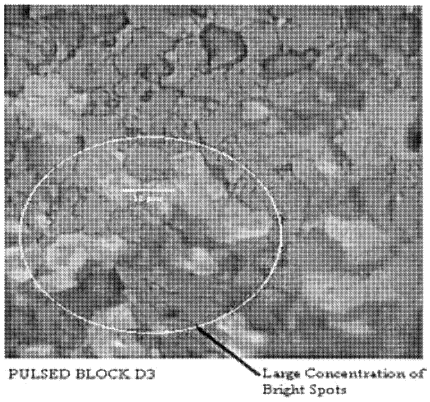

Figure 6. Un pulsed and Pulsed Block D3 under Optical Microscope.

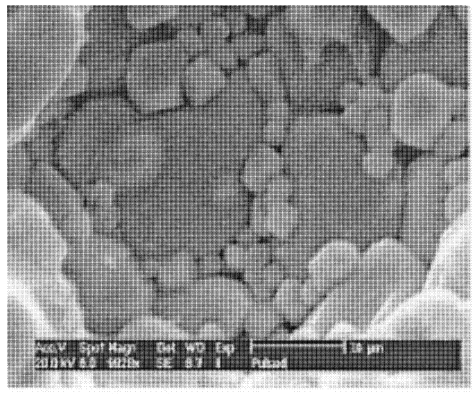

Figure 7. SEM on Pulsed Block D3.

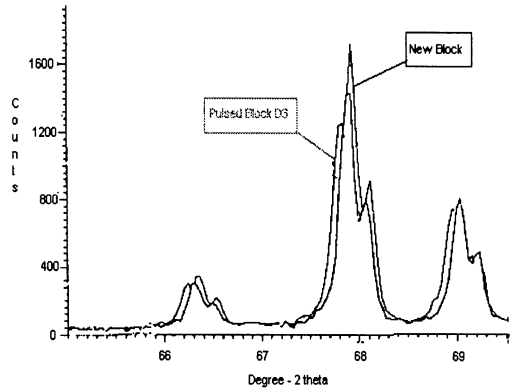

Figure 8. X-Ray Diffraction on New Block and Pulsed Block D3.

Conductivities of each arrester were calculated using equation (6) and are presented in Table 4. Table 4 shows that the conductivities for all arresters increased (1.7 % to 42.5 %) after the application of various current pulses except for arrester D4, which slightly increased. Arrester D3 again had the most significant increase in its conductivity. It increased from 1.74×10^{-12} to 2.48×10^{-12} S/m, which was about 42.5% higher compared to its original value. This increase in the dc conductivity suggests that the insulation resistance of the material is reduced.

The physical effects of the impulse current tests on the MO blocks are now presented. Using optical microscopy and scanning electron microscopy, it was found that the grain size appeared to be smaller in the pulsed specimens. The average grain size reduced from 26 to 12 μm in arrester block D3. A typical comparison is shown in Figure 6. The SEM study on arrester block D3 (as shown in Figure 7) confirmed that the average grain size was reduced. It was also observed that pulsed block D3 had a large concentration of bright spots compared to a new block.

A comparison of XRD and EDS patterns of new varistor blocks and pulsed varistor D3 was used in an attempt to examine the phase presence and intensity ratio of this grain. Figure 8, Tables 5 and 6 show this comparison.

Figure 8 shows that the relative intensities of the diffractions were almost identical; no significant changes in terms of composition and peak value were observed. However, there is an indication that the peak position had shifted. It suggests that the lattice parameters experienced some changes. In EDS observations (Tables 5 and 6), large concentrations of bismuth and small zinc elements were found on small areas of pulsed varistors compared to undegraded areas. These phenomena were most probably due to the non-uniform conduction in the blocks, creating hot spots and leading to localized degradation of the material.

5 DISCUSSIONS

Changes in 1 mA reference and discharge residual voltages were all within the allowable $\pm 5\%$ except for arrester D3. The results indicate that all arresters except D3 passed the A.S.1307.2 diagnostic test [3] even after the application of severe lightning impulse currents. However, there were some anomalies in the results. It was found that the 1 mA reference voltages for all arresters increased after being subjected to current pulses. These do not make any sense; the degraded arrester should require less voltage to force 1 mA through the arrester.

Table 5. EDS results on un-degraded area of varistor D3.

kV = 20 Tilt: 0.00
Detector type: SUTW, Sapphire
Resolution: 147.90 Lsec: 168
EDAX ZAF Quantification (Standardless)
Element Normalised
SEC Table: Default

Element	Wt%	At%	K-Ratio	Z	A	F
0 (K)	17.41	46.81	0.0521	1.1523	0.2592	1.0018
Bi (M)	2.53	0.52	0.0161	0.7705	0.8268	1.0000
Zn (K)	80.05	52.67	0.7727	0.9619	1.0020	1.0015
Total	100.00	100.00				

Legend:

Element	Net Inte.	Bkgd Inte.	Inte. Error	P/B
0 (K)	93.20	2.6	0.82	35.78
Bi (M)	11.17	20.98	5.02	0.53
Zn (K)	339.17	8.68	0.43	39.05

Table 6. EDS results on degraded area of varistor D3.

kV = 20 Tilt: 0.00
Detector type: SUTW, Sapphire
Resolution: 147.90 Lsec: 95

EDAX ZAF Quantification (Standardless)
Element Normalized
SEC Table: Default

Element	Wt%	At%	K-Ratio	Z	A	F
0 (K)	10.63	54.65	0.0201	1.2899	0.1470	1.0001
Bi (M)	77.64	30.57	0.7163	0.9025	1.0223	1.0000
ZN (K)	11.74	14.78	0.1307	1.1459	0.9342	1.0401
Total	100.00	100.00				

Legend:

Element	Net Inte.	Bkgd Inte.	Inte. Error	P/B
0 (K)	50.00	6.9	1.64	7.15
Bi (M)	688.26	33.2	0.41	20.73
Zn (K)	79.60	20.5	1.41	3.88

The return voltage results indicate clearly that the insulation condition of the MOSA changed. The reduction of their return voltages and central-time constants may explain the MOSA characteristics after the application of current pulses [9]. Arrester D3 had the biggest reduction in both return voltage and central-time constant. Its return voltage decreased more than 61 % of its initial value and reached the peak voltage in a much shorter time compared to its original. Less time to reach its peak return voltage suggests that its conductivity had increased [19, 20]. The other arresters also followed the same decreasing trend although with a lesser ratio.

The changes in conductivity shown in Table 4 implies that the V-I characteristics of the MOSA have also changed. The calculated conductivity for all arresters had increased except for arrester D4. Arrester D3 had the most

Table 7. Comparison of different diagnostic test results.

	% Change				
MOSA	1 mA Ref. voltage	Residual voltage	Return voltage	CTC	Conductivity (σ)
D1	2.3 and 3.1	−4.9	−43.8	−38.9	14.1
D2	0.8 and 2.3	−4.6	−29.5	−4.4	15.8
D3	5.3 and 6.8	−5.6	−61.3	−72.8	42.5
D4	2.3 and 3.0	−3.1	−23.8	−31.1	−1.5
S1	4.3 and 2.9	−1.7	−9.4	−37.7	6.5
S2	−1.5 and 3.0	−2.2	−9.3	−46.3	8.8
S3	1.5 and 1.5	−1.1	−14.9	−32.8	1.7
S4	3.0 and 2.9	−1.7	−2.9	−18.2	2.7

significant increase in its calculated conductivity. The increase in the calculated conductivity suggests that the insulation resistance of the material is reduced. The reduction of insulation resistance may affect the arresters ability to operate correctly when they are at normal condition (as insulators).

Table 7 compares the results from different diagnostics. The new diagnostic test results indicate that arrester D3 was the most severely degraded after the artificial degradation. This agrees with the existing diagnostic test results which show that arrester D3 had failed after the application of current pulses. These findings suggest a strong correlation between the existing techniques and the relatively new diagnostic techniques based on polarization methods.

Table 7 also suggests that the existing techniques- reference voltage and residual voltage are good tools to determine pass or fail condition of MOSA. However, they do not provide sufficient information on the level of degradation of the MOSA. Unlike the existing techniques, the new polarization test results show relatively large changes in the ratio characteristics on MOSA after the application of current pulses that could provide more information of the MOSA insulation condition.

The reduction in average grain size of MO varistors only occurred in a small area of the varistors (see Figures 4 and 5). This suggests that the reduction is mainly due to the passage of high current which is high enough to create localized hot spots leading to reduction of grain size. The local temperature required for this process is thought to be around 1000°C. This would occur if the pulse energy were concentrated in about 1.5% of the varistor volume, which appears to be feasible when the microstructure is examined.

The change in the relative intensities of the ZnO peaks and the change in concentration ratios on the pulsed varistor were observed in Figure 8, Table 5 and 6, and it is possible that phase transformation could have occurred. Several analyses of the pulsed specimens were carried out and all gave different intensity ratios. It is therefore likely that transformation exists in the pulsed samples.

The phase transformation could therefore be due to the development of local "hot spots" when a current pulse is

passed through the varistor. These high temperature regions would be areas where the conductivity is higher i.e. where large ZnO grains or some other inhomogeneity exists. The material in these hot spots forms plasma during the current pulse, but rapidly cools afterwards due to heat conduction to the surrounding zinc oxide grains. An amorphous phase is thus formed.

This phase could affect the conductivity in two ways. Firstly, if the phase has a low resistivity, then the overall resistance of the ZnO varistor would be decreased in the low voltage regions. This would lead to an increase in the leakage current, a phenomenon observed previously [21]. Alternatively, the amorphous material could provide a path for rapid oxygen diffusion. This could lead to a reduction in the meta-stable component of the potential barrier proposed by Gupta and Carlson [22, 23] and hence increase the leakage currents.

6 CONCLUSIONS

A number of non-destructive and destructive diagnostic techniques for assessing the condition of MOSA have been discussed in this paper. The results indicate a comparable degree of degradation for each of the different techniques. The new polarization techniques have shown an excellent correlation with a number of existing techniques such as 1 mA reference voltage and discharge residual voltage measurement. They have shown relatively large changes in ratio characteristics on MOSA after the application of current pulses which could provide more information of the MOSA insulation condition.

The microstructure observations showed that degraded varistors were found to have smaller average grain size, changes in the diffraction peak position and different element ratio compositions compared to new samples. A possible explanation is the non-uniform temperature distribution in the material due to the development of localized hot spots during the current impulse and the dissolving in some other phases.

The reduction in average grain size and change in the lattice parameters could affect the electrical properties by lowering the resistance and increasing capacitances of bulk material at low voltages. Hence it changes the leakage current. These findings suggest that the microstructure of a varistor has a strong correlation with its electrical characteristics. The reduction in its average grain size and larger concentration of bright spots in particular after the current pulses could significantly change the electrical characteristics of a varistor by increasing its conductivity.

In conclusion, the modern non-destructive electrical diagnostics based on polarization methods such as return voltage and polarization/depolarization current measurement have shown good indications of the ageing level of MOSA. The non-destructive diagnostics and the destructive diagnostic results obtained from this study have also proven that there is a strong correlation between electrical properties and microstructure characteristics of MOSA. Although this study was conducted on distribution class arresters, the techniques could be applied to substation class high voltage arresters. This will be performed in a continuing research project and findings will be reported in a future paper.

REFERENCES

[1] R. A. Sargent, G. L. Dunlop and M. Darveniza, "Effects of Multiple Impulse Currents on the Microstructure and Electrical Properties of Metal-oxide Varistors", IEEE Trans. Electr. Insul., Vol. 27, pp. 586–592, 1992.

[2] M. Darveniza, D. Roby, L. R. Tumma, "Laboratory and Analytical Studies of the Effects of Multipulse Lightning Current on Metal Oxide Arresters", IEEE Trans. Power Del., Vol. 9, pp. 764–71, 1994.

[3] Surge Arresters Part 2: Metal Oxide Surge Arresters without Gaps for AC Systems", Australian Standard 1307.2. 1996.

[4] "Surge Arresters Part 4: Metal Oxide Surge Arrester without Gaps for AC Systems", IEC 600099-4, Edition 1.1, 1998-08.

[5] "IEEE Standard for Metal Oxide for Alternating Current Power Circuit", ANSI/IEEE C62.11, 1993.

[6] "High-voltage Test Techniques Part 1: General Definitions and Test Requirements", Australian Standard 1931.1. 1996.

[7] U. Gafvert, "Condition Assessment of Insulation System-Analysis of Dielectric Response Methods", Nordic Insul. Sympos., NORD IS 96., Trondheim, Norway, 1996.

[8] A. K. Jonscher, *Dielectric Relaxation in Solids*, Chelsea Dielectric Press, London, UK, 1983.

[9] C. Heinrich and W. Kalkner, "Return Voltage Measurement on Metal Oxide Surge Arrester", 10th Intern. Sympos. High Voltage Engineering, Montreal, Canada, Vol. 5, pp. 137-40, 1997.

[10] A. Bognar, G. Csèpes, I. Hamos, I. Kispal and P. Osvath, "Comparing Various Methods for the Dielectric Diagnostics of Oil-Paper Insulation Systems in the Range of Long Time Constant", Proc. 8th Intern. Sympos. High Voltage Engineering, Yokohama, Japan, pp. 99–103, 1993.

[11] T. K. Saha and T. Dinh "Return Voltage Measurements on Metal Oxide Surge Arresters", Intern. Sympos. High Voltage Engineering, London, UK, Vol. 2, pp. 313–316, 1999.

[12] K. P. Mardira, M. Darveniza, T. K. Saha, "Search for New Diagnostics for Metal Oxide Surge Arrester", 6th Intern. Conf. Properties and Applications of Dielectric Materials, Xian, China, Vol. 2, pp. 947–950, 2000.

[13] K. P. Mardira, T. K. Saha and R. A. Sutton, "The Effects of Electrical Degradation on the Microstructure of Metal Oxide Varistor", IEEE/PES Transmission & Distribution Conf., Atlanta, USA, Vol. 1, pp. 329–334, 2001,

[14] K. P. Mardira, T. K. Saha, "Modern Electrical Diagnostics for Metal Oxide Surge Arresters", IEEE/PES Transmission and Distribution Conf., Yokohama, Japan, Vol. 2, pp. 672–76, 2002.

[15] C. E. Lyman, D. E. Newbury, J. Goldstein, D. B. Williams, A. D. Romig, J. Armstrong, P. Echlin, C. Fiori, D. C. Joy, E. Lifshin and K. Peters, *Scanning Electron Microscopy, X-Ray Microanalysis and Analytical Electron Microscopy: A Laboratory Workbook*, Plenum Press, New York, 1990.

[16] On the Preparation of Analytical SEM Specimens, JEOL DATUMN.

[17] C. Suryanarayana, *X-Ray Diffraction*, Plenum Press, New York, 1998.

[18] M. Darveniza, C. J. Andrews, D. R. Mercer and T. M. Parnell, "A Multiple Lightning Impulse Generator", 6th Int. Sympos. High Voltage Engineering, New Orleans, USA, paper 47.07, 1989.

[19] T. K. Saha, M. Darveniza, J. T. Hill, and T. Lee, "Electrical and Chemical Diagnostics of Transformer Insulation-Part A: Aged Transformer Samples", IEEE Trans. Power Del., Vol. 12, pp. 1547–1544, 1997.

[20] T. K. Saha, M. Darveniza, J. T. Hill, and T. Lee, "Electrical and Chemical Diagnostics of Transformer Insulation-Part B: "Accelerated Aged Insulation Samples", IEEE Trans. Power Del., Vol. 12, pp. 1555-1561, 1997.

[21] L. M. Levinson and H. R. Phillip, "Zinc Oxide Varistors - A Review", Ceramic Bulletin, Vol. 65, pp. 639–46, 1986.

[22] T. K. Gupta, "Influence of Microstructure and Chemistry on the Electrical Characteristic of ZnO Varistors", in Tailoring Multiphase and Composite Ceramics, pp. 493–507, Plenum Press, New York, 1986.

[23] T. K. Gupta and W. G. Carlson, "A Grain - Boundary Defect Model for Instability/Stability of ZnO Varistor Material", J. Appl. Phys., Vol. 20, pp. 3487–3500, 1985.

Karl Primardi Mardira was born in 1976. He graduated with a B.Eng. (Honours) degree in electrical engineering from the University of Queensland, Australia in 1998. Recently he completed his Ph.D. degree at the same university. His research interests are in power system analysis, power system protection, insulation systems and network grounding.

Tapan Kumar Saha (M'93, SM'97) was born in Bangladesh in 1959. He received the B.Sc. Eng. degree from the Bangladesh University of Engineering and Technology, Dhaka in 1982, the M.Tech. degree from the Indian Institute of Technology, Delhi, India in 1985 and the Ph.D. degree from the University of Queensland, Brisbane, Australia in 1994. Dr. Saha is an Associate Professor in the School of Information Technology and Electrical Engineering, University of Queensland, Australia. Before joining the University of Queensland in 1996 he taught at the Bangladesh University of Engineering and Technology, Dhaka, Bangladesh for three and a half years and at James Cook University, Townsville, Australia for two and a half years. Dr Saha is a Fellow and a Chartered Professional Engineer of the Institution of Engineers, Australia. His research interests include power systems, power quality, and condition monitoring of electrical plants.

Roberta Sutton graduated with a B.Eng. (Hon.) degree in manufacturing and materials engineering from the University of Queensland, Australia in 1990. She obtained the M.S. and the Ph.D. degrees from Carnegie Mellon University, USA in 1992 and 1996, respectively, and subsequently worked there doing first principle calculations. She is currently working at the University of Queensland, with research interests in computer modeling of materials, and electronic materials.